Supplemental Materials

Cereblon harnesses Myc-dependent bioenergetics and activity of CD8+ T lymphocytes

[1,2,*]Rebecca S. Hesterberg, [1,*]Matthew S. Beatty, [1,3,*]Ying Han, [4]Mario R. Fernandez, [1,2]Afua A. Akuffo, [1]William E. Goodheart, [4]Chunying Yang, [1,2] Shiun Chang, [1] Christelle M. Colin, [1]Aileen Y. Alontaga, [1]Jessica M. McDaniel, [1]Adam W. Mailloux, [1,2]Julia M. R. Billington, [1,5]Lanzhu Yue, [2,6]Shonagh Russell, [6]Robert J. Gillies, [7]Sang Y Yun, [7#]Muhammad Ayaz, [8]Nicholas J. Lawrence, [7]Harshani R. Lawrence, [9]Xue-Zhong Yu, [9]Jianing Fu, [10]Lancia N. Darville, [10,11]John M. Koomen, [3]Xiubao Ren, [12]Jane Messina, [12]Kun Jiang, [13]Timothy J. Garrett, [14]Anjali M. Rajadhyaksha, [4]John L. Cleveland, and [1]Pearlie K. Epling-Burnette

Departments of [1]Immunology, [4]Tumor Biology, [6]Cancer Physiology, [8]Drug Discovery, [11]Molecular Oncology, and [12]Anatomic Pathology and Cutaneous Oncology, Moffitt Cancer Center & Research Institute, Tampa, FL 33612, USA; [2]Cancer Biology PhD Program, University of South Florida, Tampa, FL 33620, USA; [3]Department of Immunology, Tianjin Cancer Institute and Hospital, Tianjin Medical University, Tianjin, PR China; [5]Department of Hematology, Tianjin Medical University General Hospital, 300052, China; [7]Chemical Biology Core, Moffitt Cancer Center & Research Institute, Tampa, FL, 33612, USA; [9]Department of Microbiology and Immunology, Medical University of South Carolina, Charleston, SC, 29425; [10]Proteomics and Metabolomics Core, Moffitt Cancer Center & Research Institute, Tampa, FL, 33612, USA; [13]Department of Pathology, Immunology and Laboratory Medicine, University of Florida, Gainesville, FL, 32610, USA; [14]Pediatric Neurology, Pediatrics, Weill Family Brain and Mind Research Institute; Graduate Program in Neuroscience, Weill Cornell Medical College, Cornell University, NY, 10065, USA

*These authors contributed equally to this work

[#]Current address: Department of Chemistry Quaid-e-Azam University Islamabad, Pakistan

Correspondence: John L. Cleveland, Department of Tumor Biology, H. Lee Moffitt Cancer Center & Research Institute, Tampa, FL 33612. E-mail: John.Cleveland@moffitt.org

List of Supplementary Materials

Supplemental Materials and Methods

Mouse husbandry and T cell culture

Germline *Crbn* heterozygous mice (*Crbn*$^{+/-}$)[1] were obtained from Dr. Anjali Rajadhyaksha (Cornell University) for use in these experiments. Mice were genotyped according to established methods and genotypes were confirmed by genomic PCR and western blots, as shown previously.[1]. OT1 transgenic mice[2] were bred to *Crbn*$^{-/-}$ mice for two generations to create OT1;*Crbn*$^{-/-}$ mice. C57Bl/6 and littermates of *Crbn*$^{-/-}$ mice were used as *Crbn*$^{+/+}$ controls. All genotyping primers are provided in supplemental Table 2. Stocks were maintained and bred at the H. Lee Moffitt Cancer Center and Research Institute under approved protocols by the Institutional Animal Care and Use Committee (IS00004986, IS00006088).

All T-cell experiments were conducted in RPMI supplemented with FBS, Penicillin, Streptomycin, Gentamicin, non-essential amino acids, sodium pyruvate and beta-mercaptoethanol.

Mouse ELISA

For cytokine analyses, supernatants were harvested at 48 hr for IL-2 and IL-17 and at 72 hr for TNFα, IFNγ, IL-10, and IL-4. Cytokines were quantified from standard curves by enzyme-linked immunosorbent assay (ELISA) according to the manufacturer's protocols (IL-2, Invitrogen; all others, R&D Systems).

Human T-cell Experiments

T-cells were treated with 10μM lenalidomide, pomalidomide, avadomide or JQ1 for 5 days. For Seahorse assays, CD4^{+} T-cells were removed by immunomagnetic selection prior to analysis.

Glucose uptake and flow cytometry analysis

Antibodies (all from BD, Biolegend, Tonbo biosciences or Thermo Fisher) were added at 0.2 μg per 10^6 cells in 100-μL volume FACs buffer (PBS with 2 mM EDTA, 1% FBS and 1% BSA) for 20-30 min at 4°C. The OVA and Trp2 tetramers (MBL) was used for staining of OT1 and OT1;*Crbn*$^{-/-}$ splenocytes and B16 TIL by adding 1.5-μL of the tetramer to 10^6 cells in 100-μL FACs buffer for 20 min at room temperature prior to antibody staining. Viability was determined by staining cells with Zombie Near IR dye (Biolegend), Ghost Dye 780 (Tonbo Biosciences) or Live/Dead Yellow (BD) for fixed cells, or with 7AAD and DAPI for freshly isolated cells. Proliferation of *Crbn*$^{+/+}$ and *Crbn*$^{-/-}$ T-cells by dye dilution was determined by staining cells with 5-10 μM CellTrace Violet (Thermo Fisher) for 10 min at 37°C in PBS prior to activation. Glucose uptake was analyzed by staining cells with 10 μM 2-(N-(7-Nitrobenz-2-oxa-1,3-diazol-4-yl)Amino)-2-Deoxyglucose (2-NBDG, Thermo Fisher) in PBS for 30-60 min at 37°C prior to antibody staining. MitoTracker fluorescence was analyzed by staining cells with 50 nM MitoTracker Green in PBS for 30 min at 37°C and membrane potential was analyzed by staining cells with 1nM TMRE for 30 minutes at 37°C and keeping cells in TMRE solution during flow analysis (Thermo Fisher). All data collection was performed on an LSRII or FACS Canto II (BD Biosciences) and analysis was performed on Flowjo software.

Metabolic analyses

Seahorse metabolic assays were conducted using activated *Crbn*$^{+/+}$ and *Crbn*$^{-/-}$ CD8+ T-cells or IM-treated human CD8$^+$ T-cells. Cells were plated in Seahorse base medium supplemented with 6 mM glucose and 1 mM glutamine at 10^5 T-cells per well in a 96-well Seahorse plate. Mitochondrial stress tests were used as per manufacturer's protocol. Extracellular acidification (ECAR) and oxygen consumption rates (OCR) were analyzed using Wave Software.

ATP, hexokinase enzymatic assay and NAD/NADH assays

Crbn$^{+/+}$ and *Crbn*$^{-/-}$ CD8^{+} T-cells were activated for 24 hr with anti-CD3ε and anti-CD28 and levels of ATP (Perkin Elmer), NAD/NADH (Promega) and hexokinase activity (Abcam) were determined after another 48 hr of culture as per the manufacturer's protocols.

Arginine and Glutamine uptake assays

Arginine and glutamine uptake assays were performed using *Crbn*$^{+/+}$ and *Crbn*$^{-/-}$ CD8^{+} T-cells that were activated for 24 hr. 3x10^{6} cells were suspended in 1x PBS with Ca^{2+} and Mg^{2+}/0.1% glucose and 0.2 µCi of the indicated amino acid was added and incubated at room temperature for 20 min. To stop the reaction, cells were spiked with 1x cold PBS. Cells were then washed twice with ice cold 1x PBS and subsequently lysed with 0.1% NaOH. The lysate was mixed with scintillation buffer and counts were determined with a TriCarb 2810 TR liquid scintillation analyzer (Perkin Elmer).

Quantitative PCR analysis

Cells pellets were kept in RLT Buffer (for Qiagen kit use) and at -80°C until RNA isolation. RNA was isolated as following manufacturer's protocol (Qiagen or Machery-Nagel) and kept at -20°C until quantification. RNA was converted into cDNA as per manufacturer's protocol (Bio-Rad) and 1-2 ng were used to quantify the expression of the following genes: human and mouse c-*Myc*, *Ifng* and *Crbn* by Taqman (Thermo Fisher); *Gzmb*, *Pfr1*, *Tbx21*, *EOMES*, *Slc7a1*, *Slc38a1*, S*lc1a5*, *Odc1*, *Oat*, *Srm*, and *Sms* by Sybr Green (IDT Technologies); and *B2M* by Taqman and Sybr Green. Sybr green probe sequences are provided in supplemental Table 3.

Gene set testing and pathway analyses

Unstimulated and 12 hr post-activated (5 µg/mL anti-CD3, 1 µg/mL anti-CD28, 24-well plate) T-cells from *Crbn*$^{+/+}$ and *Crbn*$^{-/-}$ mice were lysed and total RNA extracted using the iPrep Trizol Plus RNA kit. 100 ng of total RNA was amplified and labeled with biotin using the Ambion Message Amp Premier RNA Amplification Kit following the manufacturer's protocol initially described by Van Gelder et al.[3]

Hybridization with the biotin-labeled RNA, staining, and scanning of the chips on the GeneChip GCS3000 scanner followed the protocol outlined in the Affymetrix technical manual as described.[4] The oligonucleotide probe arrays used were the Mouse Genome 430 2.0 Array, which contain over 45,000 probe sets representing over 34,000 transcripts. The array output files were visually inspected for hybridization artifacts and then analyzed using Affymetrix Expression Console v 1.4 using the MAS 5.0 algorithm, scaling probe sets to an average intensity of 500. Pre-processing and normalization was then performed using Partek microarray data analysis software. Raw intensity files were processed using robust multi-array average (RMA). Principle Component Analysis (PCA) and unsupervised hierarchical clustering were performed. Statistical analysis was performed using two-way ANOVA. Gene lists with 2-fold differential expression and FDR≤0.05 between the unstimulated and activated state in *Crbn*$^{+/+}$ and *Crbn*$^{-/-}$ T-cells were compared. Gene Ontology (GO) analysis was performed on genes differentially expressed only in *Crbn*$^{-/-}$ T-cells following activation using MetaCore by GeneGo. The microarray data have been deposited to the Gene Expression Omnibus database under accession number GSE81725.

Transmission electron microscopy

Pellets from unstimulated and 24 hr stimulated T-cells were fixed immediately in cacodylate buffer (pH 7.4-7.5) with 2% glutaraldehyde overnight, and resuspended in 1% osmium tetroxide. Samples were dehydrated step-wise (50%, 70%, 95%, 100%) in increasing concentrations of alcohol followed by step-wise (2:1, 1:1, 1:2, 0:1 alcohol to resin) infiltration of resin. Resin blocks were cut on a microtome and images acquired on a JEOL 1400 transmission electron microscope. Mitochondria number and average mitochondrial length was determined by visually using Adobe Photoshop.

Western blot analyses

Cells were lysed in RIPA lysis buffer supplemented with protease (Roche Pharmaceuticals) and phosphatase (Sigma-Aldrich) inhibitors. 30-40 μg protein was separated by SDS-PAGE on 4-12%

gradient Bis-Tris gels using Novex Protein Separation System (Thermo Fisher Scientific). Antibodies were purchased from Cell Signaling Technology, Sigma Aldrich or gifted from Celgene. Densitometry was performed on 600 dpi greyscale images using ImageJ software (http://imagej.nih.gov/ij/ds) and values were normalized to β-Actin.

Homeostatic T-cell proliferation

CD45.1 mice were sublethally irradiated at 600rad and $2x10^5$ CellTrace Violet-labeled *Crbn*$^{+/+}$ and *Crbn*$^{-/-}$ T-cells were injected via tail vein. Average number of divisions (division index) and memory populations were analyzed among spleen populations on day 7 after adoptive cell transfer.

Statistical analyses

Statistical analyses for global metabolic profiling were performed separately on the positive and negative ion data, including both previously identified and unknown metabolites. Data integrity, missing data estimation, and data filtering were first performed on the data set. Normalization of the samples to allow adjustment of differences among the samples was performed using normalization by sum (*i.e.*, the total ion signal). Log transformation and autoscaling were selected. Univariate analysis by ANOVA was performed. Chemometric analysis including PCA and Partial Least Squares-Discriminant Analysis (PLS-DA) were conducted. Metaboanalyst 3.0[6] was used for statistical analysis using unpaired peak intensity tables in column format exported from MZmine.

For general statistical analyses, p-values were determined using GraphPad Prism Software (GraphPad Software) by Student's t test, Mantel-Cox Log-rank test, or two-way ANOVA as indicated in the figure legends. Equal variance was assumed between groups. All data are represented as mean with error bars representing ± standard error. Number of animals in each group is listed in the figure legends for experiments entailing biological replicates. Technical replicate experiments are representative of 2-3 independent experiments and contain 3-6 replicates. Group sizes were based on prior experience with similar studies.

General compound synthesis and verification

All reagents were purchased from commercial suppliers and used without further purification. Melting points were determined using an Optimelt automated melting point system (Stanford Research Systems) and remain uncorrected. Proton NMR spectra were recorded on an Agilent-Varian Mercury 400 MHz spectrometer or Bruker AVANCE III™ HD 500 MHz spectrometer with $CDCl_3$ or DMSO-d_6 as the solvent. Carbon (^{13}C) NMR spectra were recorded at 100 MHz or 126 MHz. All coupling constants were measured in Hertz (Hz) and the chemical shifts (δ_H and δ_C) were quoted in parts per million (ppm) relative to TMS (δ 0). Formula guided High Resolution Mass Spectroscopy (HRMS) was carried out on an Agilent G6230BA single Quad and TOF LC/MS system using a Zorbax SB-C18 rapid resolution column (2.1 × 30 mm, 3.5 μm). High Performance Liquid Chromatography and Mass Spectroscopy (HPLC-MS) were recorded on Agilent 6120 quadrupole 1220 Infinity LC/MS using a ZORBAX SB-C18 column (4.6×50 mm, 1.8 μm). HPLC analysis was performed using a JASCO HPLC system equipped with a PU-2089 Plus quaternary gradient pump and a UV-2075 Plus UV-VIS detector, using an Alltech Kromasil C-18 column (150 × 4.6 mm, 5 μm) and Agilent Eclipse XDB-C18 (150 × 4.6 mm, 5 μm). Thin layer chromatography was performed using silica gel 60 F254 plates (Fisher), with observation under UV when necessary. SiO_2 chromatography was carried out using a Biotage Isolera purification system. Anhydrous solvents (acetonitrile, dimethylformamide, ethanol, isopropanol, methanol and tetrahydrofuran) were used as purchased from Aldrich. Burdick and Jackson HPLC grade solvents (methanol, acetonitrile and water) were purchased from VWR for HPLC and high resolution mass analysis. HPLC grade TFA was purchased from Fisher. Detailed synthesis of compounds is provided in supplemental information.

Chemical Synthesis

Synthesis of CC-122

2-Methyl-5-nitro-4*H*-benzo[d][1,3]oxazin-4-one (2).[7] In a microwave reaction vial (10 mL), 2-amino-6-nitrobenzoic acid (500 mg, 2.75 mmol) and acetic anhydride (5 mL) were heated in a Biotage Initiator microwave reactor at 200°C for 30 min. After cooling, the excess acetic anhydride was evaporated to provide a dark brown solid (~550 mg) which was dissolved in EtOAc (~5 mL). Upon addition of hexane (~10 mL) and sonication, a light brown solid precipitated. The suspension was kept at 4°C for 1 hr and filtered. The residue was washed with hexane (~20 mL) and air dried to provide the title compound **2** as a beige solid (402 mg, 71%). Mp: 147-149°C, (lit. Mp: 155-156°C).[8] A second reaction using 2-amino-6-nitrobenzoic acid (1 g) in the same way furnished **2** in 89% yield. ^{1}H NMR (500 MHz, DMSO-d_6): δ 8.06 (t, J = 8.0 Hz, 1H), 7.93 (dd, J = 8.0, 1.5 Hz, 1H), 7.79 (dd, J = 8.0, 1.1 Hz, 1H), 2.42 (s, 3H).

3-(2-Methyl-5-nitro-4-oxoquinazolin-3(4*H*)-yl)piperidine-2,6-dione (3).[9] 3-Aminopiperidine-2,6-dione hydrochloride (196.3 mg, 1.19 mmol) and **2** (300 mg, 1.46 mmol) were dissolved in anhydrous pyridine (5 mL) in a microwave vial (10 ml). The vial was sealed and heated at 140°C (oil bath temperature) for 18 hr. After the reaction was complete (as monitored by TLC), the majority of the pyridine was evaporated and azeotropically removed with MeOH using a rotary evaporator. The resulting thick blackish residue was purified using SiO_2 chromatography eluting with a gradient of DCM-MeOH (0 to 20% MeOH). The title compound **3** was obtained as a light brown solid (86 mg, 23%). Mp: 284°C (dec). ^{1}H NMR (500 MHz, DMSO-d_6): δ 11.06 (s, 1H), 7.98 (t, J = 8.0 Hz, 1H), 7.87 (dd, J = 8.5, 1.0 Hz, 1H), 7.81 (dd, J = 8.0, 1.1 Hz, 1H), 5.34 (dd, J = 12.0, 5.5 Hz, 1H), 2.82 (ddd, J = 17.8, 13.2, 3.3 Hz, 1H), 2.68 (s, 3H), 2.63–2.53 (m, 2H), 2.24–2.12 (m, 1H); HPLC–MS (ESI+): *m/z* 317.2 $(M+H)^+$.

3-(5-Amino-2-methyl-4-oxoquinazolin-3(4*H*)-yl)piperidine-2,6-dione (CC-122).[9] A three-neck round bottom flask containing $Pd(OH)_2$ (20% on carbon, 77.8 mg, 0.10 equiv.) was evacuated and flushed with argon. Dry DMF (20 mL) was added and argon gas was purged though the mixture for ~10 min. The argon line was replaced with a hydrogen balloon, and **3** (350 mg, 1.11 mmol) dissolved

in DMF (3 mL) was added *via* a syringe. The reaction was stirred at room temperature under a hydrogen atmosphere for 18 hr. After confirming the reaction was complete (as monitored by TLC and HPLC-MS) the mixture was passed through a pad of celite. The filtrate was concentrated and purified by SiO_2 chromatography eluting with a gradient of DCM-MeOH (0 to 15% MeOH) to provide the title compound as a beige solid (162 mg, 51%). Mp: 264°C (dec), (lit. Mp: 295-297°C)[2]. HPLC: 97% [t_R = 11.9 min, gradient MeOH-water (with 0.1% TFA), 5-95% over 30 min.]; ^{1}H NMR (400 MHz, DMSO-d_6): δ 10.99 (s, 1H), 7.36 (t, *J* = 8.0 Hz, 1H), 7.03 (brs, 2H), 6.58 (dd, *J* = 8.0, 1.0 Hz, 1H), 6.55 (dd, *J* = 8.0, 1.2 Hz, 1H), 5.15 (dd, *J* = 11.4, 5.7 Hz, 1H), 2.90–2.75 (m, 1H), 2.68–2.57 (m, 2H), 2.53 (s, 3H), 2.18–2.08 (m, 1H); ^{13}C NMR (126 MHz, DMSO-d_6): δ 173. 61, 169.70, 162.64, 153.66, 150.59, 148.22, 134.96, 111.42, 110.53, 104.20, 55.96, 30.57, 23.20, 21.04; HPLC–MS (ESI+): *m/z* 287.2 $(M+H)^+$. HRMS (ESI+): *m/z* calcd for $C_{14}H_{15}N_4O_3$ $(M+H)^+$ 287.1139, found 287.1141.

Preparation of MYCMI-6

(*E*)-3-((9-Amino-7-ethoxyacridin-3-yl)diazenyl)pyridine-2,6-diamine: The diazonium salt of ethacridine lactate was prepared according to the reported procedure.[10] A 100 mL round bottom flask was charged with ethacridine lactate monohydrate (0.36 g, 1 mmol), H_2O (50 mL) and hydrochloric acid (1.5 mL, 3N aq.). The mixture was cooled to 0°C and a solution of $NaNO_2$ [0.1 g, 1.45 mmol, in H_2O (5 mL)] was added. Tetrafluoroboric acid (10 mL, 35% in H_2O) was subsequently added to the mixture, and stirring continued for 10 min at 0°C. The mixture was filtered. The red solid obtained was washed with cold H_2O, ethanol and Et_2O to give **SY4-046** (0.2 g, 57%). This material was used, without further purification, in the next reaction, according to a general method for coupling diazonium salts with 2,6-diaminopyridine.[11] First, 2,6-diaminopyridine (70 mg, 0.64 mmol) was dissolved in hydrochloric acid (1.0 mL, 2N aq.) and cooled to 0°C. The diazonium salt **SY4-046** (0.2 g, 0.57 mmol) was added and the mixture was stirred for 10 min. Sodium acetate (solid) was added to adjust pH (between 5 – 6) and the mixture was stirred for a further 2 min. The crude mixture was filtered and the red solid obtained was transferred to a 50 mL round bottom flask, saturated

$NaHCO_3$ solution (25 mL) was added and stirred for 20 min. The resulting mixture was filtered and the red solid was washed with cold H_2O and ethanol. The red solid was dried under vacuum to afford **SY4-047** (130 mg, 62%). HPLC: 99.7% [t_R = 14.03 min, gradient MeOH 5–95% in water (with 0.1% TFA), 20 min, 254 nm]. ^{1}H NMR (500 MHz, DMSO-d_6) J = 9.5 Hz, 1H), 7.98 (d, J = 2.0 Hz, 1H), 7.81 (d, J = 9.0 Hz, 1H), 7.75 (t, J = 9.5 Hz, 2H), 7.65 (d, J = 2.0 Hz, 1H), 7.47 (s, 2H), 7.35 (dd, J = 9.5, 2.5 Hz, 1H), 6.77 (s, 2H), 6.02 (d, J = 9.0 Hz, 1H), 4.22 (q, J = 7.0 Hz, 2H), 1.45 (t, J = 7.0 Hz, 3H). ^{13}C NMR (125 MHz, DMSO-d_6) m/z 374.2 $(M+H)^+$. HRMS (ESI+): m/z calcd for $C_{20}H_{20}N_7O$ $(M+H)^+$ 374.1724, found 374.1717.

The purity of the following compounds was determined as > 95% by HPLC-MS.

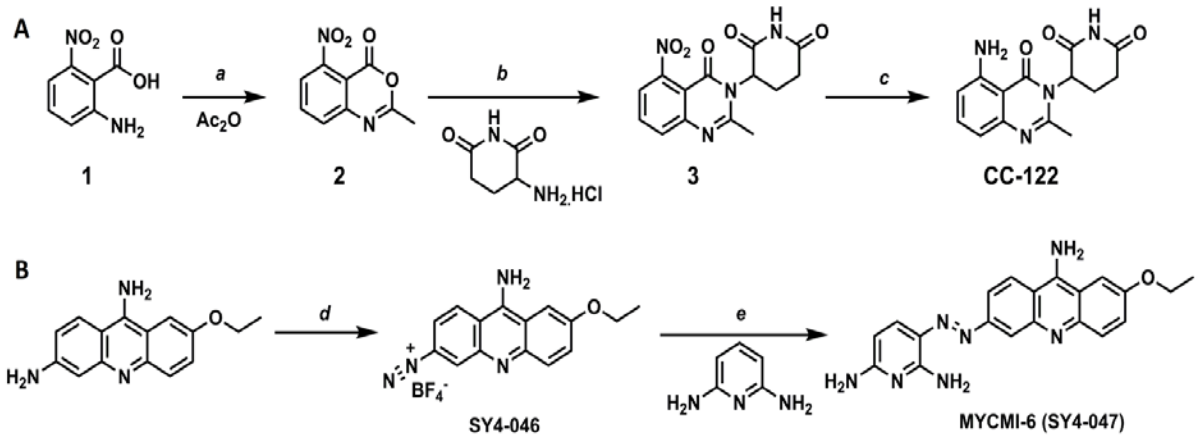

Synthesis of CC-122. *Reagents and conditions*. (a) 200 °C, 30 min, 85%; (b) Pyridine, 140 °C, 18 h, 23%; (c) $Pd(OH)_2$, H_2 (balloon), DMF, rt, 12 h, 51%.

Synthesis of MYCMI-6. *Reagents and conditions*. (d) $NaNO_2$, HCl, 0 °C; 2. HBF_4; (e) 1. 2N HCl; 2. NaOAc.

Lenalidomide (purchased from LC Laboratories); HPLC–MS (ESI+): m/z 260 $(M+H)^+$.

Pomalidomide (purchased from Ark Pharm, Inc.); HPLC–MS (ESI+): m/z 274 $(M+H)^+$.

Thalidomide (purchased from Sigma-Aldrich); HPLC–MS (ESI+): m/z 259 $(M+H)^+$.

JQ-1; HPLC–MS (ESI+): *m/z* 457 $(M+H)^+$.

10074-G5; HPLC–MS (ESI+): *m/z* 355 $(M+Na)^+$.

Quantitation of polyamines and global profiling by LC/MS

Polyamine extraction, LC/MS and quantitation

Extraction. Cell pellets (1 x 10^6 T-cells per replicate, n = 3) were spiked with 5 µL of internal standard solution containing 1 µg/mL of $^{13}C_4$-putrescine, $^{13}C_5$-ornithine, 1,1,2,2,3,3,4,4-D_8-N-(3-Aminopropyl) Butane-1,4-Diamine:3HCl (D_8-spermidine), and 1,1,2,2,3,3,4,4-D_8-N,N'-Bis(3-Aminopropyl)-1,4-Butanediamine:4HCl (D_8-spermine). An aliquot (200-µL) of HPLC grade methanol heated to 80°C was added to each sample, vortexed and incubated for 5 min at 80°C. Samples were centrifuged at 16,200 x *g* for 15 min at 4°C. The extraction process was repeated using 100-µL of hot methanol at 80°C. The supernatants containing metabolites from both extractions were pooled and dried in a vacuum centrifuge (Savant SC210A, ThermoFisher Scientific). Samples were resuspended in 50-µL of HPLC grade water.

Liquid Chromatography-Selected Ion Monitoring. Metabolomics was performed on an ultra-performance liquid chromatography (UPLC model U3000, Dionex) interfaced with an electrospray Q Exactive HF mass spectrometer (ThermoFisher Scientific) using full MS and selected ion monitoring (LC-SIM) for quantification of each target. The following solvent system is used: solvent A is 100% HPLC grade water (Burdick & Jackson, Honeywell) containing 0.05% Heptafluorobutyric acid, and solvent B is aqueous 90% acetonitrile with 0.1% formic acid. For each sample, a 10-µl aliquot of the metabolite mixture was loaded onto an Accucore reverse phase C18 column (27826-153030, 2.1 mm x 100 mm, 2.6 µm particle size, ThermoFisher Scientific). A gradient of 20% B to 80% B was applied over 6 min with a flow rate of 0.350 mL/min followed by re-equilibration over 3 min, for a total of 9 min for the LC experiment. Mass spectrometry instrument parameters for SIM on the Q Exactive HF included the following: resolution 70,000; isolation window width 1.0 *m/z* and isolation offset 0.2

m/z; AGC target 2e5; maximum IT 100 ms; an inclusion list containing the *m/z* for each metabolite, its respective stable isotope standard (SIS) and a scheduled time window for metabolite elution.

Data Analysis for Metabolite Quantification. Xcalibur Quan Browser (version 3.0.63, ThermoFisher Scientific, San Jose, CA) was used for data analysis. Metabolite amounts (pmol) were calculated using the peak area ratio of each molecule to its respective.

Global metabolomic profiling

Sample preparation. Samples were thawed on ice then centrifuged at 20,000 x *g* for 5 minutes at 4°C to pellet the cells. Supernatants were discarded and the pellets were washed with 1 mL of 40 mM ammonium formate. The samples were mixed on a vortex and then centrifuged at 20,000 x *g* for 5 minutes at 4°C and supernatants were discarded. The wash step was performed 2 more times. To each sample, 50 µL of 5 mM ammonium acetate and 10-20 pieces of 0.7 mm zirconia beads were added. Homogenization was done on a Bead Beater (BioSpec, Bartlesville, OK) at 1800 rpm for 30 sec. Samples were incubated at 4°C for 30 min. Protein concentrations were determined using Qubit Protein Assay kit. Prior to extraction, samples were normalized to 300 µg/mL or to the lowest protein concentration by diluting to 50 µL with 5 mM ammonium acetate. Each sample received 10 µL of internal standards solution, containing creatine-D3 H2O, L-Leucine-D10, L-tryptophan-2,3,3-D3, Citric acid 13C6, L-tyrosine Ring 13C6, L-tryptophan 13C11, L-leucine 13C6, L-phenylalanine Ring-13C6, N-BOC-L-tert-leucine, and N-BOC-L-aspartic acid. Samples were extracted by protein precipitation using 1 mL ice-cold 80% methanol/20% water and mixed on the Bead Beater (BioSpec Products) at 1,800 rpm for 30 sec. Further protein precipitation was allowed by incubating the samples at 4°C for 30 min. Samples were centrifuged at 20,000 x *g* for 5 min at 4°C to pellet the protein. An aliquot of the supernatant (1 mL) was transferred from each sample into clean tube and dried under a gentle stream of nitrogen at 30°C. Dried extracts were re-suspended with 30 µL reconstitution solution consisting of injection standards in 0.1% formic acid in water containing 6

μg/mL of Boc-L-tyrosine, Boc-L-tryptophan, and Boc-D-phenylalanine. Resuspension was allowed at 4°C for 10 -15 minutes; then, samples were centrifuged at 20,000 x *g* for 5 minutes at 4°C. Supernatants were collected into clean LC-vials for LC-MS metabolomics analysis.

LC-MS Global metabolomics. Profiling was performed on a Thermo Q-Exactive Orbitrap mass spectrometer with Dionex UHPLC and autosampler. All samples were analyzed with positive and negative heated electrospray ionization with a mass resolution of 35,000 at m/z 200 as separate injections. Sheath gas and auxiliary gas flow rates were set at 50 and 10, respectively, with auxiliary gas temperature of 350°C. Spray voltage was set to 3.0 kV and capillary temperature to 325°C. Mass range was from m/z 70 to 1000 with MS acquisition for 17.5 min. Separation was achieved on an ACE 18-PFP 100 x 2.1 mm, 2 μm column (MAC-MOD Analytical, Chadds Ford, PA) with mobile phase A as 0.1% formic acid in water and mobile phase B as acetonitrile. The flow rate was 350 μL/min with a column temperature of 25°C. Total LC run time was 20.5 min. The initial condition of 100% A at 0.35 mL/min was held for 3 min then a linear gradient from 0-80% B for 10 min. To wash the column, 80% B was held for 3 min before going back to 0% B. For each sample, 4 μL was injected for negative ion analysis and 2 μL for positive ions.

Data processing. Data from positive and negative ion modes were processed separately. LC-MS files were first converted to open-format files (i.e. MzXML) using MSConvert (Proteowizard 3.0.10095). MZmine 2.23 was used to identify features, deisotope peaks, align features and perform gap filling to fill in any features that may have been missed in the first alignment algorithm.[12] All adducts and complexes were identified and removed from the data set prior to statistical analysis.

Statistical analyses were performed separately on the positive and negative ion data including both previously identified and unknown metabolites. Metaboanalyst 3.0[6] was used for statistical analysis using unpaired peak intensity tables in column format exported from MZmine. Data integrity, missing data estimation, and data filtering were first performed on the data set. Normalization of the samples to allow adjustment of differences among the samples was performed

using normalization by sum (*i.e.*, total ion signal). Log transformation and autoscaling were selected. Univariate analysis by ANOVA was performed. Chemometric analysis including Principal Component Analysis (PCA) and Partial Least Squares-Discriminant Analysis (PLS-DA) were conducted. Unsupervised clustering with visualization in a heat map was also done on the data set. Statistical analysis is provided in the main manuscript.

B16-OVA cytotoxicity assay

B16-OVA target cells (gift from Dr. S Pilon-Thomas, Moffitt Cancer Center) were treated with 10ng/mL of IFNγ for 2 hours at 37°C and re-plated in a flat-bottom 96-well plate. Activated OT1 and OT1;*Crbn*$^{-/-}$ were then added at a 5:1 T cell to target ratio for 6 hr. LDH release in the media as per manufacturer's protocol and percent of target cells lysed was determined by the following equation:

$$\frac{Experimental\ LDH - T\ cell\ spontaneous\ LDH - B16OVA\ spontaneous\ LDH}{B16OVA\ total\ LDH - B16OVA\ spontaneous\ LDH} x100$$

CRBN CRISPR/Cas9 editing

Guide crRNA's targeting 2 locations of CRBN (AACTACTCCGGGCGGTTACC and CAGGACGCTGCGC ACAACAT) were manufactured on Integrated DNA Technologies's Alt-R platform. Negative crRNA guides that do not target the human genome were also purchased through IDT. Lyophilized guides were resuspened at 100μM in IDT duplex buffer. Guide crRNA's were then duplexed with tracrRNA (IDT) in equimolar ratio at 95°C for 5 min before gradual cooling to room temperature. Complexed guide RNA's were then incubated for 15 min at room temperature with purified CAS9 protein (Invitrogen TrueCut CAS9 v2, Cat# A36499) at a ratio of 3:1 (Guide RNA : CAS9) by adding 3uL of guide RNA to 2μL of CAS9 protein. Following incubation, complexed RNP (Guide RNA + CAS9) was mixed with 4 x 10^6 CD8+ T-cells that had been resuspended in 15μL Lonza P2 Primary cell solution (Lonza, Cat# PBP2-00675). RNP cell mixture was then transferred into the provided nucleocuvette

strip and nucleoporated on a Lonza Amaxa 4-D-Nucleofector using pulse code EH100. Following nucleoporation, cells were immediately transferred to warm media and rested for 48 hr for downstream assays

Supplemental Figure Legends

Supplemental Figure 1. (A) CRBN protein levels are dynamically regulated in human T-cells following stimulation with anti-CD3 and anti-CD28. Actin served as a loading control. (B) Unsupervised clustering of transcripts from unstimulated and 12 hr anti-CD3ε/anti-CD28 activated *Crbn*$^{+/+}$ and *Crbn*$^{-/-}$ purified T-cells (unstim *Crbn*$^{+/+}$, n=3; unstim *Crbn*$^{-/-}$, n=2; activated *Crbn*$^{+/+}$, n=3; and activated *Crbn*$^{-/-}$, n=3). (C) Crbn protein levels in T-cells (D) and *Crbn* mRNA levels in the indicated mouse immune tissues or immune cell subsets derived from spleens of *Crbn*$^{+/+}$ (+) or *Crbn*$^{-/-}$ (-) mice, normalized to mRNA encoding Tata binding protein (*TBP*). (E) Percent CD4^{+} and CD8^{+} T-cells among total CD3^{+} splenocytes in 3 month old *Crbn*$^{+/+}$ and *Crbn*$^{-/-}$ mice. (F) CD44 expression on CD8^{+} and CD4^{+} T-cells in aging *Crbn*$^{+/+}$ and *Crbn*$^{-/-}$ mice. (G) Levels of TNFα, IL-17, IL-10 and IL-4 in activated pan T-cells from *Crbn*$^{+/+}$ and *Crbn*$^{-/-}$ mice. (H) Western blot analysis of Ikaros, CK1α, IRF-4, and β-actin in unstimulated and anti-CD3ε/anti-CD28 activated *Crbn*$^{+/+}$ and *Crbn*$^{-/-}$ T-cells. (I) mRNA levels of *IKZF1* in *Crbn*$^{+/+}$ and *Crbn*$^{-/-}$ T-cells and of (J) *Prf1* in *Crbn*$^{+/+}$ and *Crbn*$^{-/-}$ CD8^{+} T-cells, following activation with anti-CD3ε/anti-CD28. n.s.=not significant, *p<0.05, **p<0.01, ***p<0.001, ****p<0.0001.

Supplemental Figure 2. Results of Agilent Seahorse XF Cell Mito Stress Test to measure (*left*) extracellular acidification rates (ECAR) and (right) oxygen consumption rates (OCR) in 24 hr anti-CD3ε or anti-CD3ε + anti-CD28-treated *Crbn*$^{+/+}$ and *Crbn*$^{-/-}$ CD8^{+} T-cells. Lines indicate addition of oligomycin to inhibit ATPase (Complex V), carbonyl cyanide-4 (trifluoromethoxy) phenylhydrazone (FCCP) to uncouple the electron transport chain for calculation of Spare Respiratory Capacity (SRC), and rotenone/antimycin to inhibit Complex I and Complex II, respectively.

Supplemental Figure 3. (A-B) Metabolomics analysis of CD8^{+} *Crbn*$^{+/+}$ and *Crbn*$^{-/-}$ T-cells 24 hr after anti-CD3ε + anti-CD28 activation. (A) Pathway analysis of metabolite abundance highlighting

statistical information for the arginine and proline metabolism pathways. (B) Principle component analysis of metabolites measured in positive mode (*left*) and negative mode (*right*). (C) Structure of the polyamines putrescine, spermidine, and spermine. (D-E) qRT-PCR analysis of the expression of the indicated amino acid transporters and enzymes that direct (D) glutamine and arginine catabolism and (E) polyamine synthesis in *Crbn*$^{+/+}$ and *Crbn*$^{-/-}$ T-cells without activation or following 24 hr stimulation with anti-CD3ε and anti-CD28 (fold change are provided in Figure 3B). (F) Spare respiratory capacity (SRC) of 24 hr activated *Crbn*$^{+/+}$ and *Crbn*$^{-/-}$ CD8^{+} T-cells. (G) Mitotracker Green staining of naïve and 24- and 72-hr activated *Crbn*$^{+/+}$ and *Crbn*$^{-/-}$ CD8^{+} T-cells. (H) Mitochondrial membrane potential of 24-hr activated *Crbn*$^{+/+}$ and *Crbn*$^{-/-}$ CD8^{+} T-cells. (I-K) Transmission electron microscopy of *Crbn*$^{+/+}$ and *Crbn*$^{-/-}$ CD8+ T-cells 24 hr after activation (I); number of mitochondria (J); and (K) average mitochondrial length. (L) Intracellular ROS (*left*) and mitochondrial ROS (*right*) levels in *Crbn*$^{+/+}$ and *Crbn*$^{-/-}$ CD8^{+} T-cells 24 hr after activation. n.s.=not significant, *p<0.05, **p<0.01, ***p<0.001, ****p<0.0001.

Supplemental Figure 4. (A) Top 10 up-regulated transcription factor drivers identified by GSEA altered in activated *Crbn*$^{-/-}$ T-cells (from data in Figure 2D) indicate pathway enrichment for Myc:Max and Myc. (B) Cell size of anti-CD3/anti-CD28 activated *Crbn*$^{+/+}$and *Crbn*$^{-/-}$ CD8^{+} T-cells. (C-D) qRT-PCR analysis of the effects of co-treatment with the indicated Myc:Max dimerization inhibitors on the expression of the indicated Myc target genes *Slc38a1*, *Slc1a5*, *Srm*, and *Sms*, and (D) on the expression of the indicated T_E genes, including*Tbx21*, *Eomes*, *Gzmb* and *Ifng*, in anti-CD3/anti-CD28 activated *Crbn*$^{+/+}$and *Crbn*$^{-/-}$ CD8^{+} T-cells. n.s.=not significant, **p<0.01, **p<0.001, ****p<0.0001.

Supplemental Figure 5. (A) The percent IL-17- and IL-5-producing T-cells from sublethally irradiated Balb/C recipient mice that received adoptive transfers of *Crbn*$^{+/+}$ and *Crbn*$^{-/-}$ T-cells. (B) H&E histochemistry analyses of skin, colon and liver from representative mice in the GVHD

model. Arrows indicate immune infiltrates and areas of pathology. (C) Schematic of experimental design to assess potential effects of *Crbn* deficiency reconstitution after homeostatic proliferation. *Crbn*$^{+/+}$ and *Crbn*$^{-/-}$ CD45.2^{+} T-cells were adoptively transferred into syngeneic sublethally-irradiated CD45.1^{+} mice. (D-E) Average number of divisions of the adoptively transferred CD4^{+} (D) and CD8^{+} (E) T cells as determined by CellTrace Violet dilution. (F) Number of splenocytes after adoptive cell transfer (ACT) over time. (G-H) Percent of naïve (CD44^{Neg}CD62L^{+}), Effector (CD44^{+}CD62L^{Neg}), and Central Memory (CD44^{+}CD62L^{+}) subsets of (G) CD4^{+} T cells and (H) CD8^{+} T cells from *Crbn*$^{+/+}$ (solid line) and *Crbn*$^{-/-}$ (dotted line) mice. n.s. = not significant.

Supplemental Figure 6. (A) Secretion of IFNγ in unstimulated and vehicle (DMSO) *vs.* avadomide (Ava)-treated cells activated with increasing doses of anti-CD3 (1, 3, and 5) µg/mL with a constant level of anti-CD28 for 72 hr. (B) IKAROS protein levels determined by flow cytometry in unstimulated and anti-CD3/anti-CD28 activated human CD8^{+} T-cells from a three healthy donor (treated with vehicle (DMSO) or IM compounds for 5 days. IM compounds were tested at 10 µM and include lenalidomide (Len), pomalidomide (Pom) and avadomide (Ava). Data shown is percentage of cells based on gating of CD8^{+} T-cells. (C) MYC protein levels in unstimulated (Unstim) and anti-CD3/anti-CD28 activated human CD4^{+} T-cells treated with vehicle or IM compounds for 5 days as detected by flow cytometry. IM compounds were tested at 10 µM and include Len, Pom and Ava. JQ1 (BET-inhibitor) was used to show staining specificity for Myc in these experiments; results are represented as geometric mean fluorescent intensity (G-MFI). (D) Expression of CD98 as detected by flow cytometry in CRISPR control (Ctrl), CRISPR-*CRBN* knockdown (CRBN KO) and 10µM Ava-treated CRISPR control (Ava) human CD8^{+} T-cells. n.s.=not significant; *, $p<0.05$.

Figure S7. Visual Abstract. Overview of signaling events harnessed by cereblon (CRBN) in activated $CD8^+$ T-cells. TCR signaling events increase ERK1/2 expression and activation, which is necessary for activation-induced increases in the levels of Myc mRNA and protein. The MYC:MAX heterodimer transcriptionally induces metabolic gene programs, such as glycolysis, glutaminolysis, and polyamine biosynthesis, and that support activated $CD8^+$ T-cells and the induction of T_E-related genes. By studying *Crbn*-deficient $CD8^+$ T-cells and the effect of modulating compounds, Lenalidomide (Len), pomalidomide (Pom) and avadomide (Ava), we demonstrate that CRBN represses the ERK1/2-MYC circuit that drives metabolism and effector function of activated $CD8^+$ T-cells. TCR = T-cell receptor, ERK1/2 = extracellular regulated kinase 1/2.

Supplemental Table 1. Key resources.

REAGENT or RESOURCE	SOURCE	IDENTIFIER
Antibodies		
CRBN	Celgene Corp	n/a
c-Myc	Cell Signaling Technology	#5605
IKZF1	Cell Signaling Technology	#5443
CK1α	Cell Signaling Technology	#2655
IRF4	Cell Signaling Technology	#4948
β-actin-peroxidase	Sigma	#A3854
Monoclonal Anti-Actin antibody produced in mouse	Sigma	#A4700
CD3e Monoclonal Antibody (145-2C11), Functional Grade	ThermoFisher	#16-0031-81
CD28 Monoclonal Antibody (37.51), Functional Grade	ThermoFisher	#16-0281-81
CD3 Monoclonal Antibody (HIT3a), Functional Grade	ThermoFisher	#16-0039-81
CD28 Monoclonal Antibody (CD28.2), Functional Grade	ThermoFisher	#16-0289-85
pMyc (T58)	Abcam	#ab28842
CD69-PE-CF594	BD Biosciences	Clone: H1.2F3
CD3, mouse, multiple fluorochromes used	Biolegend, BD Biosciences or Tonbo	Clone: 17A2
CD3-APC, human	Tonbo	Clone: UCHT1
B220, mouse, multiple fluorochromes used	BD Biosciences or Biolegend	Clone: RA3-6B2
CD19,mouse, multiple fluorochromes used	Biolegend or Invitrogen	Clone: 6D5
Granzyme B PE-Cy7	Invitrogen	Clone: NGZB
NK1.1, mouse	BD Biosciences	Clone: PK136
CD8α, mouse, multiple fluorochromes used	Biolegend, Tonbo or BD	Clone:53-6.7 or 2.43
CD4, mouse, multiple fluorochromes used	Biolegend, BD Biosciences or Tonbo	Clone: GK1.4 or RM4-5
CD25-APC, mouse	Tonbo	Clone: PC61.5
Vα2-PE, mouse	eBioscience	Clone: B20.1
Vβ5-FITC, mouse	eBioscience	Clone: MR9-4
CD98-PE, mouse	Biolegend	Clone: RL388

CD98-PE, human	BD Biosciences	Clone: UM7F8
CD44-BV510	Biolegend	Clone: IM7
CD127-PE-Cy7, mouse	Biolegend	Clone: A7R34
KLRG1-BV421, mouse	Biolegend	Clone: 2F1/KLRG1
IFNγ	BD Biosciences	Clone: XMG1.2
IL-17A	BD Biosciences	Clone: TC11-18H10.1
IL-5	BD Biosciences	Clone: TRFK5
c-Myc, human/mouse, multiple colors used	Cell Signaling Technology	Clone:D84C12
Foxp3, multiple fluorochromes used	eBioscience	Clone: FJK-16s
PD1-PE	Tonbo	Clone: J43.1
Biological Samples		
Human PBMCs	One Blood, St Petersburg, FL	N/A
Chemicals, Peptides, and Recombinant Proteins		
OVA (257-264)	Anaspec	#AS-60193-1
OVA-A2 Peptide, SAINFEKL, OVA (257-264) Variant	Anaspec	#AS-64383
OVA-G4 Peptide, SIIGFEKL, OVA (257-264) Variant	Anaspec	#AS-64384
TRP - 2 (180 - 188)	Anaspec	#AS-61058
Recombinant Murine IL-2	Peprotech	#212-12
Recombinant Murine IFNγ	Peprotech	#315-05
2-Deoxy-D-glucose	Sigma	#D8375
Oligomycin A	Sigma	#75351
$^{13}C_4$-putrescine	Cambridge Isotope Labs	# CLM-6574
$^{13}C_5$-ornithine	Cambridge Isotope Labs	#CLM-4724
1,1,2,2,3,3,4,4-D_8-N-(3-Aminopropyl) Butane-1,4-Diamine:3HCL	Cambridge Isotope Labs	#DLM-9262
1,1,2,2,3,3,4,4-D8-N,N'-Bis(3-Aminopropyl)-1,4-Butanediamine:4HCL	Cambridge Isotope Labs	#DLM-9262
HPLC Grade Water	Honeywell Chemicals	#AH3654
HPLC Grade Methanol	Honeywell Chemicals	#AH2304
HPLC Grade Acetonitrile	Honeywell Chemicals	#AH0154
Formic Acid	Thermo Fisher	#PI28905
Accucore C18 Column 150 x 3.0 mm, 2.6 µm	Thermo Fisher	#27826-153030
Ionomycin	Thermo Fisher	#I24222
Fluo4AM	Thermo Fisher	#F14217
Thapsigargin	Thermo Fisher	#T7428

Heptafluorobutyric acid	ProteoChem	#LC6206
Hyaluronidase V	Sigma	#H6254
Collagenase type I	Sigma	#SCR103
Collagenase type IV	Sigma	#C5138
DNAse I	Sigma	#DN25
JQ-1	Sigma	#SML0974
10074-G5	Sigma	#G3798
RIPA buffer	Sigma	#R0278
Calcium Chloride	Sigma	#C4901
MycMI-11 (NSC 11656)	NCI	
Recombinant Mouse IL-2 Protein	R&D Systems	#402
L-TYROSINE (RING-$^{13}C_6$, 99%)	Cambridge Isotope Labs	#CLM-1542
L-TRYPTOPHAN ($^{13}C_{11}$, 99%)	Cambridge Isotope Labs	#CLM-4290-H-PK
L-LEUCINE ($^{13}C_6$, 99%)	Cambridge Isotope Labs	#CLM-2262-H-PK
L-PHENYLALANINE (RING-$^{13}C_6$, 99%)	Cambridge Isotope Labs	#CLM-1055-0
N-BOC-L-tert-Leucine, 98%	Acros Organics	#368010010
N-BOC-L-Aspartic acid, 99%	Acros Organics	#303210010
BOC-L-Tyrosine, 99+%	Acros Organics	#275700050
Nalpha-BOC-L-Tryptophane, 97%	Acros Organics	#275690050
BOC-D-Phenylalanine, 99+%	Acros Organics	#275740050
Creatine-d_3 H_2O (methyl-d_3)	CDN isotopes	#D-1972
D-Leucine-d_{10}	CDN isotopes	#D-5607
L-Tryptophan-2,3,3-d_3	CDN isotopes	#D-7419
Water with 0.1% Formic Acid (v/v), Optima™ LC/MS Grade	Fisher Scientific	#LS1184
Citric acid ($^{13}C_6$, 99%)	Cambridge Isotope Labs	#CLM-9021
GLUTAMINE, L-[14C(U)]	American Radiolabeled Chemicals	#ARC0196-50
PD98059	Caymen Chemical	#10006726
Arginine L-[14C(U)]	Perkin Elmer	#NEC267E050UC
Critical Commercial Assays		
IFN gamma Mouse ELISA Kit	ThermoFisher	#KMC4022
Seahorse XF Cell Mito Stress Test Kit	Agilent	#103015-100
Mouse IL-2 Recombinant Protein, eBioscience	Invitrogen	#14-8021-64
Mouse IL-17 Quantikine ELISA Kit	R&D systems	#M1700
Mouse IL-10 Quantikine ELISA Kit	R&D systems	#M1000B
Mouse TNF-alpha Quantikine ELISA Kit	R&D systems	#MTA00B
Mouse IFN-gamma Quantikine ELISA Kit	R&D systems	#MIF00
Mouse IL-4 Quantikine ELISA Kit	R&D systems	#M4000B
Human IFNg ELISA Ready-Set-Go	eBioscience	#88-7316-88

Pierce™ LDH Cytotoxicity Assay Kit	Thermo Fisher	#88953
Hexokinase Activity Assay Kit (Colorimetric)	Abcam	#ab136957
NAD/NADH-Glo™ Assay	Promega	#G9071
GeneChip™ Mouse Genome 430 2.0 Array	Thermo Fisher	#900495
Qubit Protein Assay Kit	Thermo Fisher	#Q33211
MessageAmp™ Premier RNA Amplification Kit	Thermo Fisher	#AM1792
ATPlite Luminescence Assay System, 300 Assay Kit	Perkin Elmer	#6016943
Deposited Data		
Microarray data	Gene Expression Omnibus	GSE81725
Experimental Models: Organisms/Strains		
C57Bl6	Jackson	#000664
CD45.1	Jackson	#002014
OT1	Jackson	#003831
BALB/cJ	Jackson	#000651
Crbn$^{-/-}$		N/A
Oligonucleotides		
Mm00487804_m1 *Myc*	ThermoFisher	#4331182
Mm01182414_m1 *Crbn*	ThermoFisher	#4351372
Mm00437762_m1 *B2m*	ThermoFisher	#4331182
Mm00446971_m1 *Tbp*	ThermoFisher	#4331182
Mm01168134_m1 *Ifng*	ThermoFisher	#4331182
Mm00434599_s1 *Kcna3*	ThermoFisher	#4331182
RT-PCR Primers (Supplemental Table)	IDT	N/A
Genotyping primers (Supplemental Table)	IDT	N/A
Software and Algorithms		
Graphpad V7	GraphPad Software	
Flowjo V10	BD	
Metaboanalyst 4.0	http://www.metaboanalyst.ca/	
Xcalibur Quan Browser	Thermo Fisher	
Partek	Partek, Inc.	
Gene Go	Thomson Reuters	
ImageJ	http://imagej.nih.gov/ij/	
MZmine	http://mzmine.github.io/	
MSConvert	http://proteowizard.sourceforge.net/	
Wave version 2.6	Agilent Technologies	
Other		
Pan T cell Isolation Kit II, mouse	Miltenyi	#130-095-130
CD8a+ T cell Isolation Kit, mouse	Miltenyi	#130-104-075

CD4+ T cell Isolation Kit, mouse	Miltenyi	#130-104-454
B cell Isolation Kit, mouse	Miltenyi	#130-090-862
CD3e Microbead Kit, mouse	Miltenyi	#130-094-973
EasySep™ Mouse T Cell Isolation Kit	Stemcell	#19851
RosetteSep Human T cell Enrichment Cocktail	Stemcell	#15061
EasySep, Human CD8+ T cell Isolation Kit	Stemcell	#17953
CD4 Microbeads, human	Miltenyi	#130-045-101
Leukocyte Activation Cocktail, with BD GolgiPlug™	BD Biosciences	#550583
CellTrace Violet	Molecular Probes	#C34557
iTAgiTAg Tetramer/PE – H-2 Kb OVA (SIINFEKL)	MBL	#T0300
2-NBDG (2-(N-(7-Nitrobenz-2-oxa-1,3-diazol-4-yl)Amino)-2-Deoxyglucose)	Molecular Probes	#N13195
Zombie NIR	Biolegend	# 423105
Ghost Dye Red 780	Tonbo	#13-0865-T500
MitoTracker Green	Thermo Fisher	# M7514
CellROX Green Reagent for oxidative stress detection	Thermo Fisher	#C10444
MitoSOX Red Mitochondrial Superoxide Indicator	Thermo Fisher	#M36008
7-AAD	BD Biosciences	#559925
DAPI (4',6-Diamidino-2-Phenylindole, Dihydrochloride)	Thermo Fisher	#D1306
Live/Dead Yellow	Molecular Probes	#L34959
CD3 Microbead Kit	Miltenyi	#130-094-973
Power SYBR™ Green PCR Master Mix	Thermo Fisher	#4367659
Taqman Universal PCR Master Mix	Thermo Fisher	#4304437
iPrep™ Trizol™ Plus RNA Kit	Thermo Fisher	#IS10007
eBioscience™ Foxp3 / Transcription Factor Staining Buffer Set	Thermo Fisher	#00-5523-00
iScript™ Reverse Transcription Supermix for RT-qPCR	Bio-Rad	#1708841
RNeasy Plus Mini Kit	Qiagen	#74134
NucleoSpin RNA	Macherey-Nagel	#740955.250
RPMI Media	Thermo Fisher	#11875
Zirconia Beads	Biospec Products	#11079107zx
Corning Cell-Tak Cell and Tissue Adhesive	Fisher Scientific	#40240
iTAg Tetramer/APC - H-2 Kb TRP2 (SVYDFFVWL)	MBL	#T03015

Supplemental Table 2. Primers for genotyping mice by genomic PCR

Mouse strain	**Primer**	**Sequence 5'-3'**
Crbn$^{-/-}$	*Loxf* (Wild-type forward primer)	AGGAGCACTGAACGGCTTACAG
Crbn$^{-/-}$	*f* (knockout forward primer)	TTGTTTCAGAACTGCTGGGATGTG
Crbn$^{-/-}$	*LoxR* (common reverse primer)	CGCATGCTGACTGATCACAGC

Supplemental Table 3. Primers for RT-PCR analyses

Gene	**Sequence 5'-3'**
Slc7a1 Forward	TGGTCTTGTGCTTCATCGTG
Slc7a1 Reverse	GACACCAGAGAATCCAAAGGG
Slc38a1 Forward	TTACCAACCATCGCCTTC
Slc38a1 Reverse	ATGAGAATGTCGCCTGTG
Slc38a2 Forward	GGTATCTGAACGGTGACTATCTG
Slc38a2 Reverse	TCTGCGGTGCTATTGAATGC
Granzyme B Forward	TGCTGCTAAAGCTGAAGAGTAAG
Granzyme B Reverse	CGTGTTTGAGTATTTGCCCATTG
T-bet Forward	CCTGGACCCAACTGTCAACT
T-bet Reverse	AACTGTGTTCCCGAGGTGTC
Eomes Forward	TACGGCCAGGGTTCTCCGCTCTAC
Eomes Reverse	GGGCCGGTTGCACAGGTAGACGTG
Perforin Forward	GCAGCTGAGAAGACCTATCAGGAC
Perforin Reverse	TCTGAGCGCCTTTTTGAAGTC
B2M Forward	TTCTGGTGCTTGTCTCACTGA
B2M Reverse	CAGTATGTTCGGCTTCCCATTC
Odc1 Forward	GACGAGTTTGACTGCCACATC
Odc1 Reverse	CGCAACATAGAACGCATCCTT
Oat Forward	GGAGTCCACACCTCAGTCG
Oat Reverse	CCACATCCCACATATAAATGCCT
Srm Forward	ACATCCTCGTCTTCCGCAGTA
Srm Reverse	GGCAGGTTGGCGATCATCT
Sms Forward	CACAGCACGCTCGACTTCAA
Sms Reverse	TGCCATTCTTGTTCGTGTAAGTT

Supplemental Table 4. Distribution of immune cells in *Crbn*$^{-/-}$ mice

	Crbn$^{+/+}$		*Crbn*$^{-/-}$		
Population name	***Mean (SD)***	***n***	***Mean (SD)***	***n***	***P-value***
Thymic Populations					
• CD4^{+} (SP)	16.5 (4.6)	11	14.7 (4.5)	9	0.39
• CD8^{+} (SP)	5.4 (2.6)	11	4.7 (2.3)	9	0.52
• CD4^{+}/CD8^{+} (DP)	65.1 (14.2)	11	63.1 (13.7)	9	0.77
• CD4^{-}/CD8^{-} (DN)	13.0 (7.2)	11	14.6 (9.2)	9	0.69
• DN1	10.2 (2.5)	11	11.8 (3.0)	9	0.25
• DN2	7.9 (5.1)	11	6.3 (4.9)	9	0.51
• DN3	51.0 (12.9)	11	53.1 (13.4)	9	0.74
• DN4	31.0 (6.9)	11	28.9 (6.4)	9	0.51
Splenic Lymphocytes					
• B220+ CD3- B cell	32.8 (8.5)	11	33.5 (16.5)	11	0.90
• B220- CD3^{+} T cells	45.9 (6.7)	11	36.4 (7.1)	11	***0.004***
• B220^{-}CD3^{-}NK1.1^{+} NK cells	18.8 (6.2)	11	19.4 (10.9)	11	0.87
• CD3^{+}CD8^{+} T cells	25.7 (5.1)	11	29.7 (8.9)	11	0.21
• CD3^{+}CD4^{+} T cells	62.3 (15.8)	11	65.4 (10.2)	11	0.58
• CD3^{+}CD4^{+}CD25^{+}Foxp3^{+} T reg cells	9.7 (0.7)	3	10.8 (4.9)	3	0.71
• CD3^{+}CD4^{+}CD69^{+} T cells	6.0 (1.7)	11	5.1 (0.9)	11	0.17
• CD3^{+}CD8^{+}CD69^{+} T cells	4.6 (0.8)	11	3.8 (1.0)	11	***0.05***
• CD3^{+}CD4^{+}CD25^{+} T cells	4.2 (0.7)	11	4.7 (0.9)	11	0.09
• CD3^{+}CD8^{+}CD25^{+} T cells	0.5 (0.6)	11	0.7 (0.8)	11	0.55
Lymph Node Lymphocytes					
• B220- CD3^{+} T cells	77.9 (6.9)	11	77.4 (6.9)	11	0.85
• B220^{-}CD3^{-}NK1.1^{+} NK cells	22.8 (18.1)	11	27.7 (15.8)	11	0.50
• CD3^{+}CD8^{+} T cells	32.8 (10.5)	11	36.0 (11.8)	11	0.51
• CD3^{+}CD4^{+} T cells	65.7 (10.2)	11	62.3 (11.6)	11	0.47
• CD3^{+}CD4^{+}CD25^{+}Foxp3^{+} Treg cells (n=3)	10.5 (0.8)	11	10.3 (0.7)	3	0.72
• CD3^{+}CD4^{+}CD69^{+} T cells	6.6 (0.8)	11	6.9 (0.7)	11	0.35
• CD3^{+}CD8^{+}CD69^{+} T cells	4.6 (0.9)	11	5.0 (1.0)	11	0.41
• CD3^{+}CD4^{+}CD25^{+} T cells	4.0 (1.0)	11	4.8 (1.2)	11	0.11
• CD3^{+}CD8^{+}CD25^{+} T cells	0.5 (0.5)	11	0.5 (0.3)	11	0.93
Splenic Memory Populations					
CD3^{+}CD4^{+}CD44^{-}CD127^{+}KLRG1^{-} T cells	70.8 (4.0)	7	69.4 (5.1)	7	0.56
CD3^{+}CD4^{+}CD44^{+}CD127^{+}KLRG1^{-} T cells	11.4 (2.3)	7	11.0 (1.4)	7	0.72
CD3^{+}CD4^{+}CD44^{+}CD127^{-}KLRG^{+} T cells	0.2 (0.1)	7	0.2 (0.1)	7	0.23
CD3^{+}CD8^{+}CD44^{-}CD127^{+}KLRG1^{-} T cells	74.8 (3.2)	7	75.6 (2.9)	7	0.63
CD3^{+}CD8^{+}CD44^{+}CD127^{+}KLRG1^{-} T cells	14.4 (3.9)	7	13.9 (1.6)	7	0.73
CD3^{+}CD8^{+}CD44^{+}CD127^{-}KLRG1^{+} T cells	0.3 (0.1)	7	0.6 (0.4)	7	0.08

Supplemental Table 5. Statistical comparisons, in reference to Figure 7

Function	Population	Comparison	Sample size	P-value	Summary
Glucose uptake (2-NBDG, gMFI)	$CD8^+$ T-cells	DMSO vs Len	3 technical	<0.0001	*****
		DMSO vs Pom	3 technical	<0.0001	*****
		DMSO vs CC122	3 technical	<0.0001	*****
	$CD8^+$ T-cells 10074-G5 10 µM	DMSO vs DMSO+10074-G5 (impact of Myc suppression on activated human T-cells)	3 technical	0.5891	n.s.
		Len vs Len+10074-G5	3 technical	>0.9999	n.s.
		Pom vs Pom+ 10074-G5	3 technical	>0.9999	n.s.
		CC122 vs CC122+10074-G5	3 technical	0.3599	n.s.
	$CD8^+$ T-cells 10074-G5 30 µM	DMSO vs DMSO+10074-G5	3 technical	>0.9999	n.s.
		Len vs Len+10074-G5	3 technical	<0.0001	*****
		Pom vs Pom+ 10074-G5	3 technical	<0.0001	*****
		CC122 vs CC122+10074-G5	3 technical	<0.0001	*****
FCS-A Mean (x100)	$CD8^+$ T-cells	Unstimulated vs stimulated (not shown)	3 technical		
		DMSO vs Len	3 technical	<0.0001	*****
		DMSO vs Pom	3 technical	<0.0001	*****
		DMSO vs CC122	3 technical	0.0034	**
	$CD8^+$ T-cells treated with 10074-G5 10 µM	DMSO vs DMSO+10074-G5	3 technical	0.5987	n.s.
		Len vs Len+10074-G5 10µM	3 technical	<0.0001	*****
		Pom vs Pom+ 10074-G5 10µM	3 technical	0.0010	**
		CC122 vs CC122+10074-G5 10µM	3 technical	0.0012	**
	$CD8^+$ T-cells treated with 10074-G5 30 µM	DMSO vs DMSO+10074-G5	3 technical	0.0066	**
		Len vs Len+10074-G5	3 technical	<0.0001	*****
		Pom vs Pom+ 10074-G5	3 technical	<0.0001	*****
		CC122 vs CC122+10074-G5	3 technical	<0.0001	*****

SUPPLEMENTAL REFERENCES

1. Rajadhyaksha AM, Ra S, Kishinevsky S, et al. Behavioral characterization of cereblon forebrain-specific conditional null mice: a model for human non-syndromic intellectual disability. *Behav Brain Res*. 2012;226(2):428-434.
2. Hogquist KA, Jameson SC, Heath WR, Howard JL, Bevan MJ, Carbone FR. T cell receptor antagonist peptides induce positive selection. *Cell*. 1994;76(1):17-27.
3. Van Gelder RN, von Zastrow ME, Yool A, Dement WC, Barchas JD, Eberwine JH. Amplified RNA synthesized from limited quantities of heterogeneous cDNA. *Proc Natl Acad Sci U S A*. 1990;87(5):1663-1667.
4. Warrington JA, Nair A, Mahadevappa M, Tsyganskaya M. Comparison of human adult and fetal expression and identification of 535 housekeeping/maintenance genes. *Physiol Genomics*. 2000;2(3):143-147.
5. Valenzuela JO, Iclozan C, Hossain MS, et al. PKCtheta is required for alloreactivity and GVHD but not for immune responses toward leukemia and infection in mice. *J Clin Invest*. 2009;119(12):3774-3786.
6. Xia J, Wishart DS. Using MetaboAnalyst 3.0 for Comprehensive Metabolomics Data Analysis. *Curr Protoc Bioinformatics*. 2016;55:14.10.11-14.10.91.
7. Muller, G.; Man, H.-W.; Cohen, B. M.; Li, Y.; Xu, J.; Leong, W. W. Solid forms of 3-(5-Amino-2-methyl-4-oxo-4H-quinazolin-3-yl)piperidine-2,6-dione, *US Patent App.*, US2012/232100(A1),(2012**).**
8. Bogert T. M.; Chambers J. V. The synthesis of 5-nitro-4-ketodihydroquinazolines from 6-nitro-2-aminobenzoic acid, 6-nitro-2-acetylaminobenzoic acid, and from the corresponding nitroacetylanthranil. *JACS* **27**, 649-658 (1905).
9. Muller, G. W.; Man, H.W. 5-Substituted quinazolinone derivatives and compositions comprisingand methods of using the same. *PCT Pat. App.*, WO2008039489(A2) (2008**)**.
10. Möhrle, H.; Lieck-Waldheim, U. V. D.; Martin, H. D.; Possberg, N.; Beutner, S. Reaction ofethacridine lactate with ntrous and the colour-structure relationships with acridine derivatives.Part 3: Analytics of ethacridine lactate. *Pharmazie* **52**, 603–611 (1997).
11. Timmis, G. M.; Felton, D. G. I. , Collier H.O.J, Haskinson P.L. Structure-activity relations in twonew series of antifolic acids. *J. Pharm. Pharmacology* **9**, 46–67 (1957).
12. Pluskal T, Castillo S, Villar-Briones A, Oresic M. MZmine 2: modular framework for processing, visualizing, and analyzing mass spectrometry-based molecular profile data. *BMC Bioinformatics*. 2010;11:395.

Supplemental Figure 1

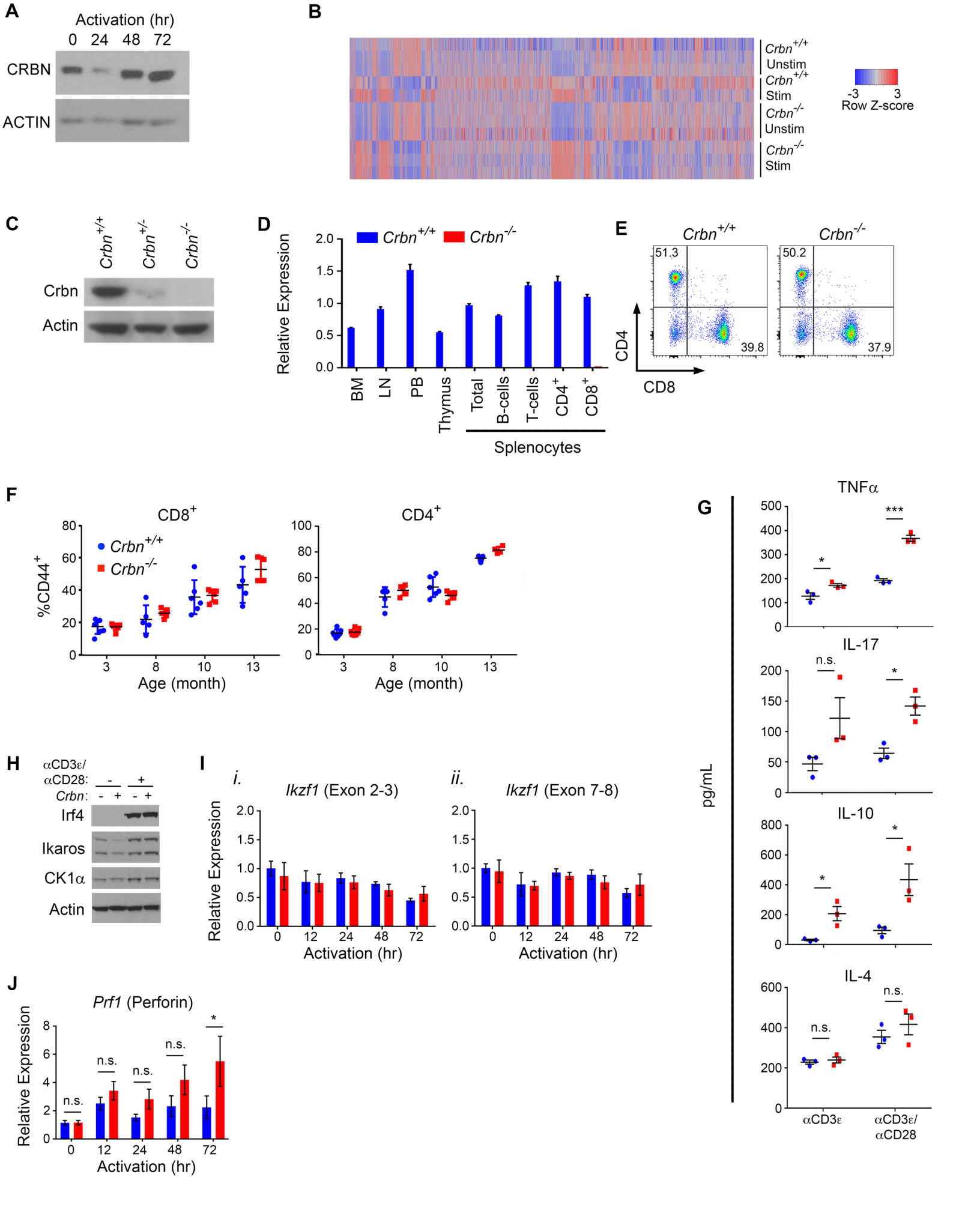

Supplemental Figure 2

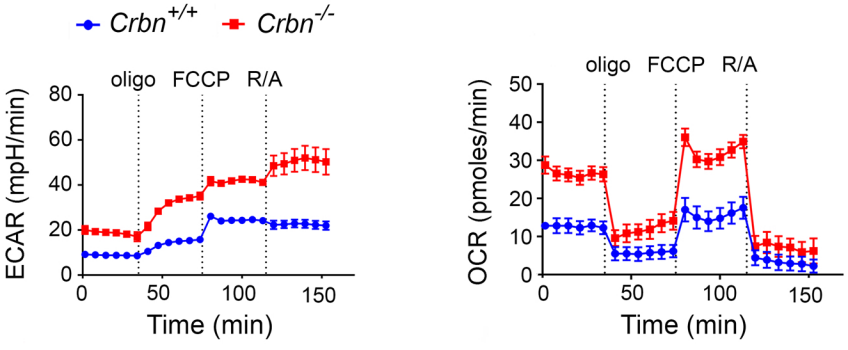

Supplemental Figure 3

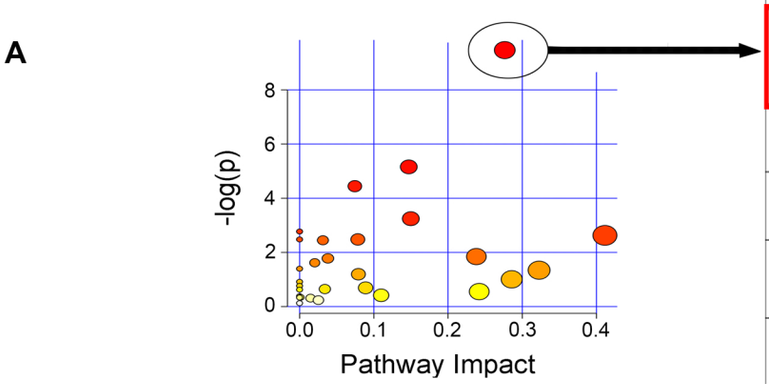

Pathway Name	Total	Hits	-log(p)	FDR	Impact
Arginine and proline metabolism	44	10	9.4675	0.0063407	0.27634
Pyrimidine metabolism	41	7	5.1582	0.23584	0.14705
Glutathione metabolism	26	5	4.445	0.32083	0.07442
Alanine, aspartate and glutamate metabolism	24	4	3.2457	0.78681	0.14979
beta-Alanine metabolism	17	3	2.773	0.78681	0

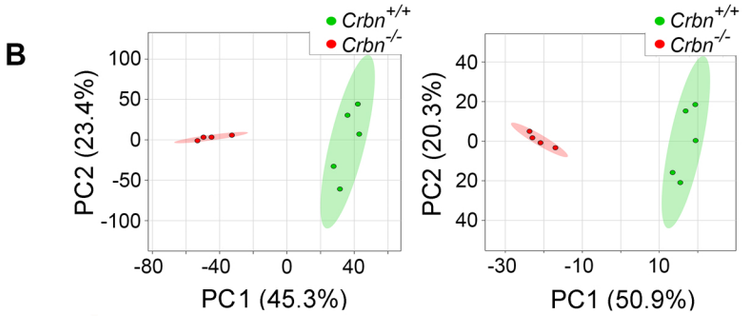

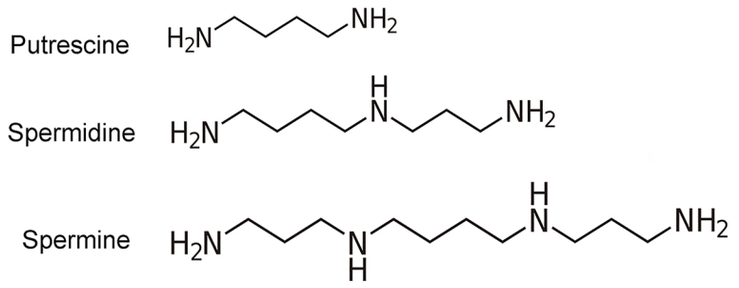

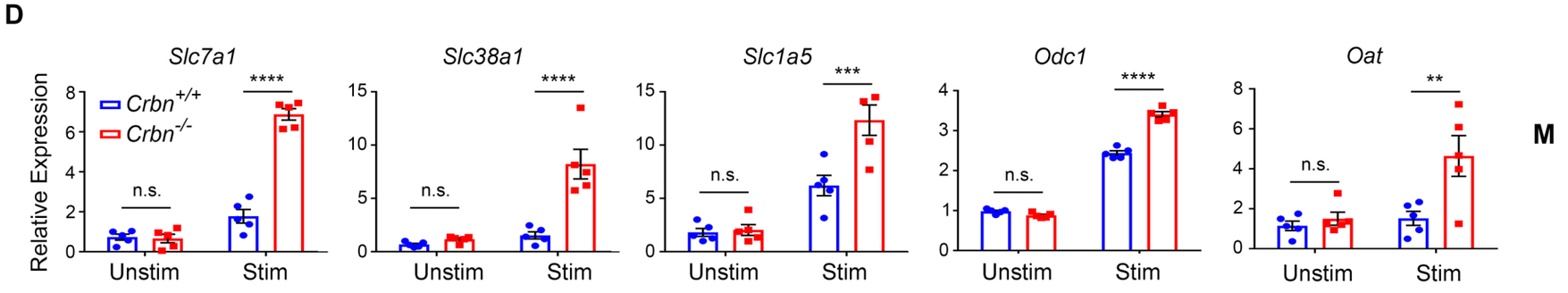

M

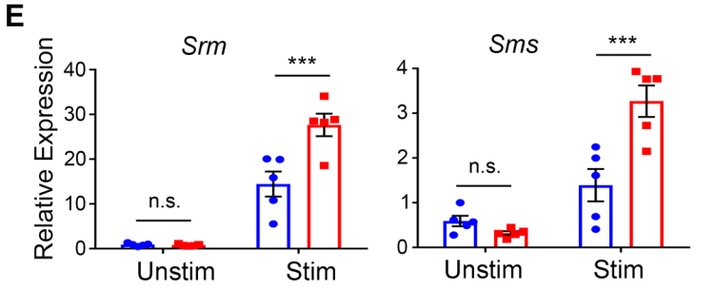

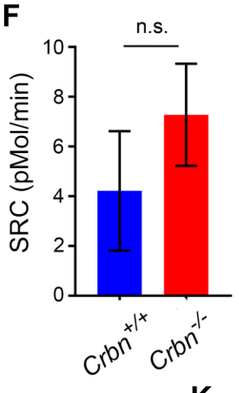

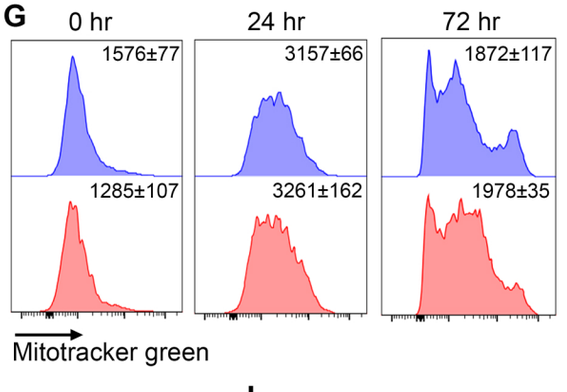

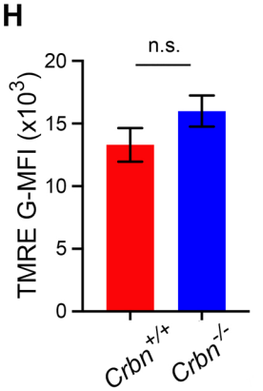

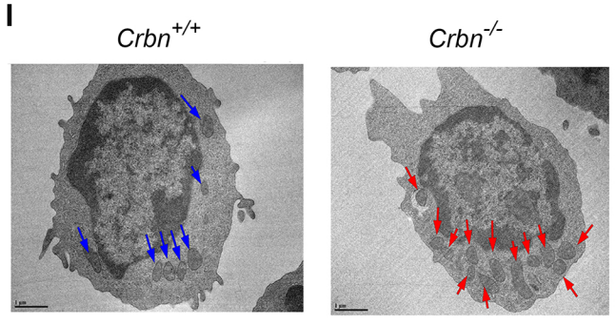

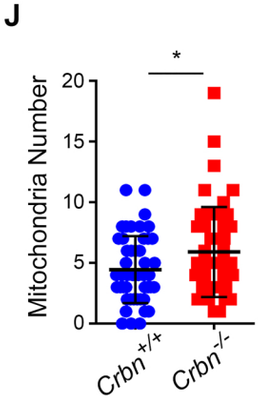

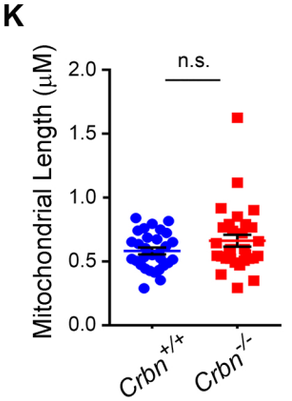

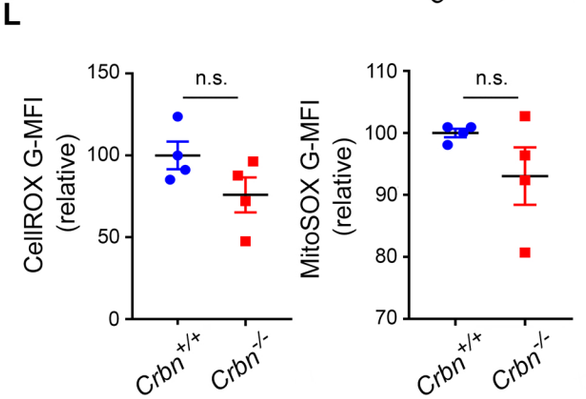

Supplemental Figure 4

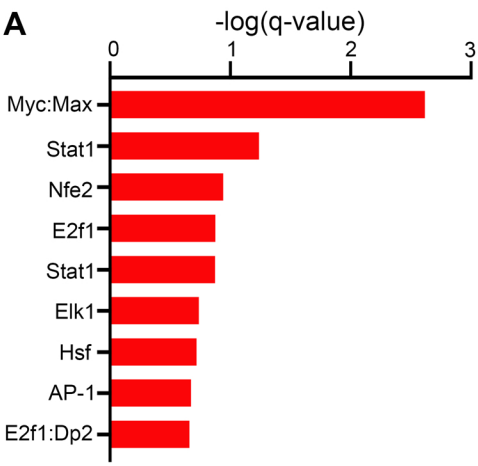

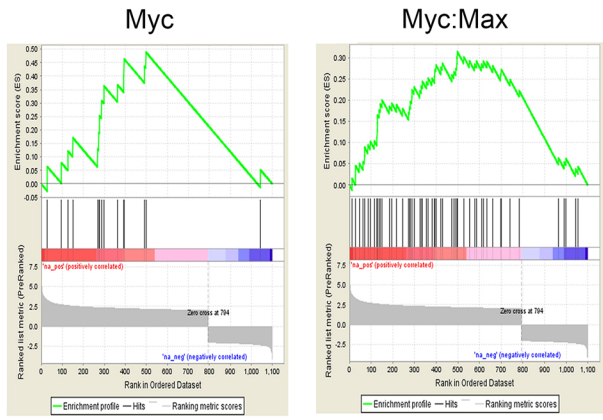

FDR q-val 0.002

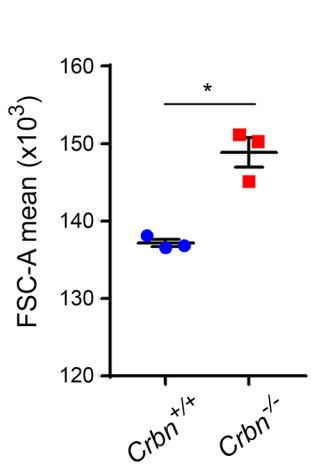

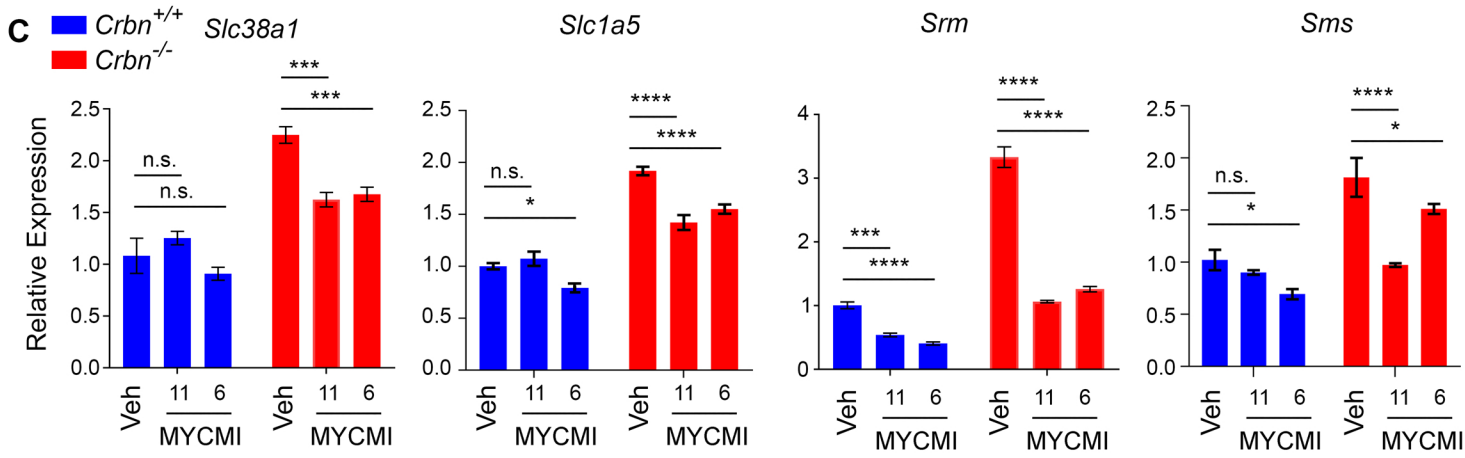

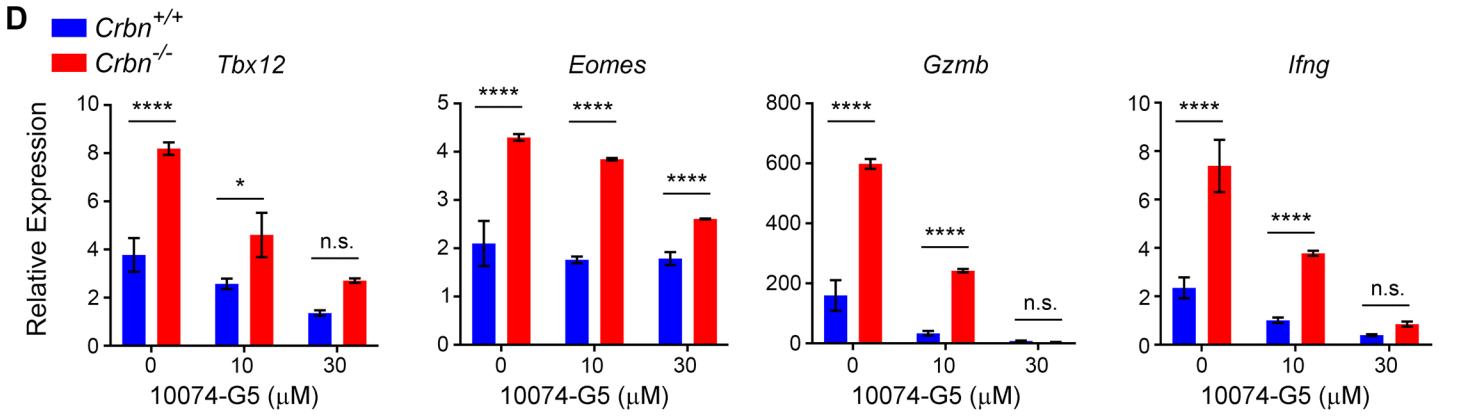

Supplemental Figure 5

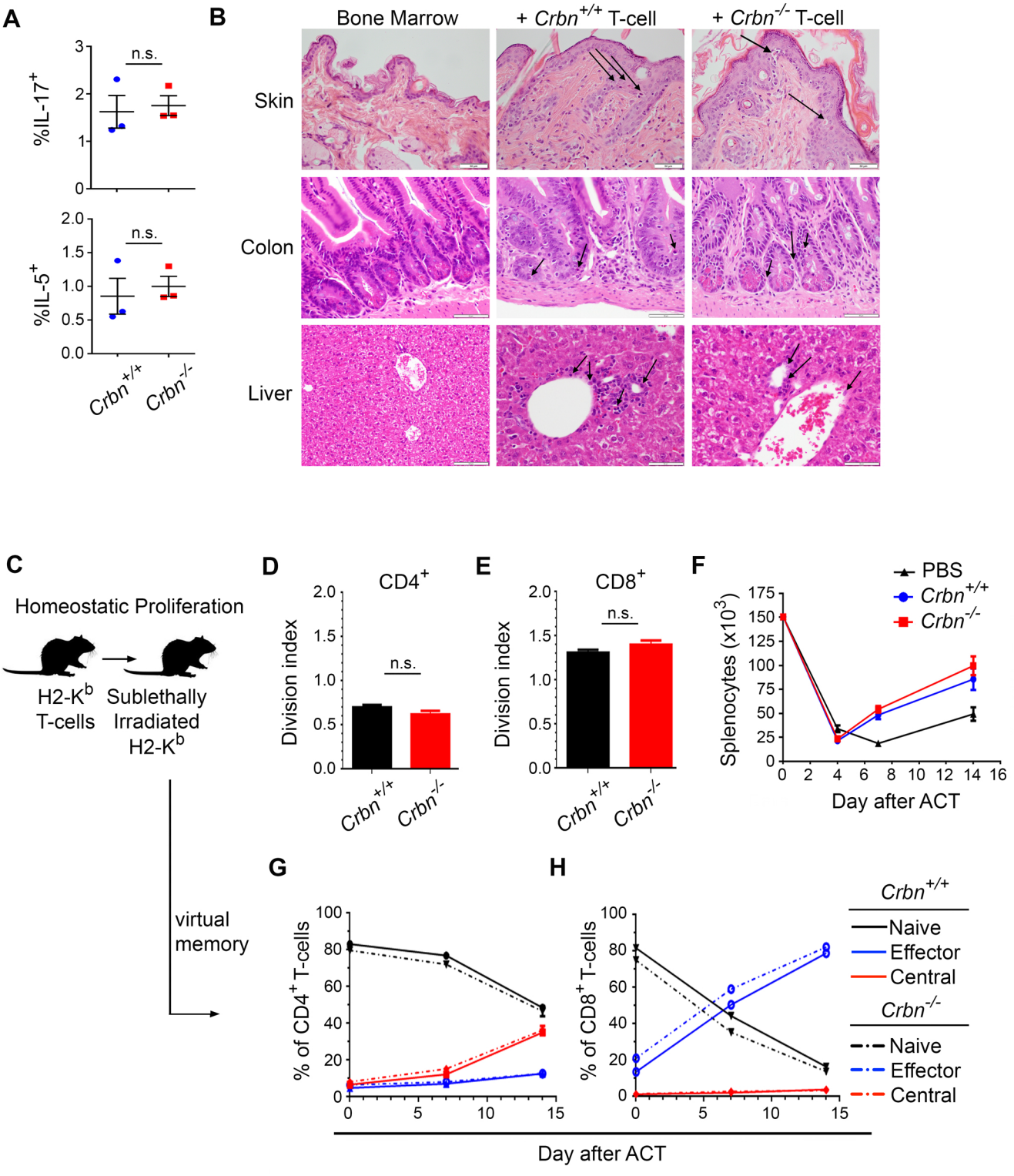

Supplemental Figure 6